

A refined stretched-vortex model for large-eddy simulation of turbulent mixing layers

T. W. Mattner

School of Mathematical Sciences
The University of Adelaide, South Australia 5005, Australia

Abstract

Some simple modifications to the stretched-vortex model are proposed. The first of these eliminates the need for calculating estimates of the resolved second-order structure function, which can be complicated on distorted or irregular grids. The second modification improves estimates of subgrid-scale spectra and associated integral quantities by equating the energy dissipation calculated from the model spectrum with the energy transfer from resolved to subgrid scales.

Introduction

Turbulent flows are characterised by irregular unsteady three-dimensional fluid motion over a wide range of spatial and temporal scales. Prediction of many turbulent flows by direct numerical simulation remains impracticable due to the enormous computational resources needed to resolve all relevant scales. This problem is mitigated in a large-eddy simulation (LES) because only the large-scale features of the flow are resolved, while the fine-scale subgrid features are modelled.

The stretched-vortex model [9, 13, 11, 4, 2, 3] is one of many models intended for large-eddy simulations. One of the capabilities of this model is the systematic prediction of subgrid-scale quantities, including the subgrid-scale spectra and associated integral quantities such as the subgrid-scale variance [4, 2].

Recently, it has been found that the original procedures developed for computing subgrid-continued spectra produce results that are grid-dependent [3]. The problem is illustrated in Figure 1, which shows one-dimensional energy spectra from large-eddy simulations of a turbulent temporal shear-layer calculated by the present author using procedures developed by Hill *et al.* [4] (hereafter referred to as the original model). The figure shows both resolved spectra and modelled subgrid extensions from simulations with different effective resolutions. The spectra are scaled in terms of Kolmogorov variables and should collapse at high wave-number but it is clear that the high wave-number subgrid extensions are resolution dependent. Using simple scaling arguments, it can be shown that the original model implies

$$\frac{\lambda_\nu}{\eta} \sim \left(\frac{\Delta}{\eta}\right)^{1/3}, \quad (1)$$

where λ_ν is the predicted viscous length-scale, Δ is the grid spacing, $\eta = (\nu^3/\epsilon)^{1/4}$ is the Kolmogorov length-scale and ϵ is the energy dissipation rate.

Although this problem has very little effect on the resolved-scale flow, it may be important if subgrid quantities are of direct interest, as is the case in combustion problems or scalar mixing, for example. Furthermore, plotting spectra with subgrid extensions is a useful way of verifying that the model implementation is working as intended.

The principal aim of this paper is to modify the original model of Hill *et al.* [4] in order to eliminate grid resolution effects. The paper begins by recapping the original model, which is identical to that used by Hill *et al.* [4] except for the subgrid-vortex

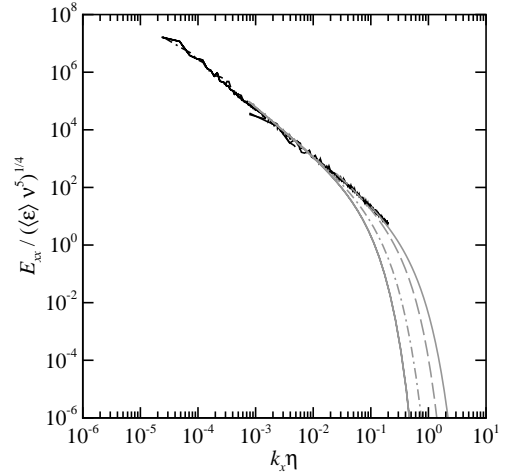


Figure 1: Resolved-scale (black) and subgrid-continued (grey) one-dimensional energy spectra for four different grid resolutions: $\Delta/\eta = 16$ (solid line), 64 (long-dash line), 503 (dot-dash line) and 2082 (dotted line).

alignment model which follows that of Kosovic *et al.* [5]. This is the model that was used to produce the spectra in Figure 1. Two modifications to this model are described, both of which make use of expressions for the local energy dissipation rate. The first modification is introduced as a convenient alternative to structure-function matching and appears to work just as well. The second modification involves matching the dissipation calculated from the model spectrum with the transfer of energy from resolved to subgrid scales. Although Chung & Pullin [3] have already devised a procedure to eliminate grid-resolution effects, the method developed here is slightly different. It is shown that the present modification leads to a model estimate of the viscous length-scale λ_ν that scales with the Kolmogorov length-scale as required. This is verified by plotting spectra from large-eddy simulations of a temporal shear-layer at different effective resolutions.

Original model

The governing equations for large-eddy simulation of an incompressible flow are

$$\frac{\partial \bar{u}_j}{\partial x_j} = 0, \quad (2a)$$

$$\frac{\partial \bar{u}_i}{\partial t} + \frac{\partial \bar{u}_i \bar{u}_j}{\partial x_j} = -\frac{\partial \bar{p}/\rho}{\partial x_i} + \frac{\partial \bar{\tau}_{ij}}{\partial x_j} - \frac{\partial T_{ij}}{\partial x_j}, \quad (2b)$$

where x_i and u_i are the components of the Eulerian position and velocity vectors, respectively, p is the pressure, τ_{ij} is the viscous stress tensor given by

$$\tau_{ij} = \nu \left[\frac{\partial u_i}{\partial x_j} + \frac{\partial u_j}{\partial x_i} \right] \quad (3)$$

and ν is the kinematic viscosity. In the derivation of the governing equations, overbars denote the filtering operation

$$\bar{f} = \int G(x-x')f(x')dx', \quad (4)$$

where G is a filter kernel. It is assumed that the filtered variables correspond to the resolved-scale quantities obtained in an actual LES. The additional term,

$$T_{ij} = \overline{u_i u_j} - \bar{u}_i \bar{u}_j, \quad (5)$$

is the subgrid stress.

The stretched-vortex subgrid stress model of Misra & Pullin [9] is used to close equation (2b). The subgrid stress is

$$T_{ij} = K(\delta_{ij} - e_i^v e_j^v) \quad (6)$$

where K is the subgrid kinetic energy per unit mass, and e_i^v are the components of a unit vector which is aligned with the subgrid vortex axis. The subgrid kinetic energy is

$$K = \int_{k_c}^{\infty} E(k) dk, \quad (7)$$

where k is the wave-number, $k_c = \pi/\Delta$ is the cut-off wave-number, $E(k)$ is the spectrum of the Lundgren spiral vortex,

$$E(k) = \mathcal{K}_0 \varepsilon^{2/3} k^{-5/3} e^{-\lambda_v^2 k^2}, \quad (8)$$

\mathcal{K}_0 is the Kolmogorov prefactor, ε is the local cell-averaged dissipation rate, $\lambda_v^2 = 2\nu/(3|a|)$, $a = e_i^v e_j^v \bar{S}_{ij}$ is the axial strain along the subgrid vortex axis [13] and \bar{S}_{ij} is the resolved rate-of-strain tensor. The group $\mathcal{K}_0 \varepsilon^{2/3}$ is calculated from the local resolved spherically-averaged second-order velocity structure function \bar{F}_2 using

$$\mathcal{K}_0 \varepsilon^{2/3} = \frac{\bar{F}_2}{A \Delta^{2/3}}, \quad (9)$$

where $A = 4 \int_0^\pi u^{-5/3} \left(1 - \frac{\sin u}{u}\right) du \approx 1.90695$ [8, 13, 11]. The resolved-scale structure function is estimated at the point x using

$$\bar{F}_2 = \frac{1}{6} \sum_{j=1}^3 (\delta \bar{u}_1^{+2} + \delta \bar{u}_2^{+2} + \delta \bar{u}_3^{+2} + \delta \bar{u}_1^{-2} + \delta \bar{u}_2^{-2} + \delta \bar{u}_3^{-2})_j \quad (10)$$

where $\delta \bar{u}_i^\pm = \bar{u}_i(x \pm e_j \Delta) - \bar{u}_i(x)$ and e_j is the unit vector in the j -th direction [4]. Subgrid vortices are assumed to align either with the principal extensional eigenvector of the resolved rate-of-strain tensor, \bar{S}_{ij} , or the resolved vorticity vector, ω . The respective proportions are given by λ and $(1-\lambda)$, where

$$\lambda = \frac{\lambda_3}{\lambda_3 + \|\omega\|} \quad (11)$$

and λ_3 is the principal extensional eigenvalue [5].

Modifications

An alternative method for calculating the group $\mathcal{K}_0 \varepsilon^{2/3}$ can be derived from the local energy balance [9],

$$\varepsilon = 2\nu \bar{S}_{ij} \bar{S}_{ij} + \varepsilon_{\text{sgs}}, \quad (12)$$

where ε is the dissipation rate and ε_{sgs} is the subgrid dissipation rate. These quantities are related to the energy spectrum $E(k)$ by

$$\varepsilon = 2\nu \int_0^\infty k^2 E(k) dk \quad \text{and} \quad \varepsilon_{\text{sgs}} = 2\nu \int_{k_c}^\infty k^2 E(k) dk, \quad (13)$$

$c_1 = 0.3032514285768450$	$c_4 = 0.4519713785569435$
$c_2 = 0.4138264302025380$	$c_5 = 0.4660579752458206$
$c_3 = 0.4314020733116885$	$c_6 = 0.4736114577011807$

Table 1: Coefficients of the six-term asymptotic expansion (19).

in which case

$$\bar{S}_{ij} \bar{S}_{ij} = \int_0^{k_c} k^2 E(k) dk. \quad (14)$$

The integral in equation (14) is evaluated by assuming that $E(k) = \mathcal{K}_0 \varepsilon^{2/3} k^{-5/3}$, in which case

$$\mathcal{K}_0 \varepsilon^{2/3} = \frac{4}{3} \frac{\bar{S}_{ij} \bar{S}_{ij}}{k_c^{4/3}}. \quad (15)$$

The form of the spectrum used in the above calculation is consistent with the model spectrum (8), provided that k_c lies within the inertial range, but it is not strictly applicable at resolved wave-numbers, $k < k_c$. On the other hand, the integral is dominated by the form of the spectrum for wave-numbers close to k_c , where the model spectrum is likely to be satisfactory. A similar issue arises in the derivation of equation (9). Voekl *et al.* [13] argue that a more detailed description of the energy spectrum is not necessary because only the integral enters into the model. A potential advantage of equation (15) over equation (9) is that it is unnecessary to calculate the resolved-scale structure-function (10), which may be complicated on irregular or distorted computational grids. Only existing computational infrastructure (i.e. calculating derivatives) is needed.

An alternative method for calculating the rate-of-strain parameter a can be derived by assuming that

$$\varepsilon_{\text{sgs}} = -\bar{S}_{ij} T_{ij}. \quad (16)$$

The quantity $-\bar{S}_{ij} T_{ij}$ is more correctly interpreted as the transfer of kinetic energy from resolved to subgrid scales. However, this quantity is often used as a surrogate for the subgrid dissipation. Substituting equation (6) into the right-hand-side of equation (16) yields $\varepsilon_{\text{sgs}} = K \bar{a}$, where $\bar{a} = e_i^v e_j^v \bar{S}_{ij}$. Note that \bar{a} is the resolved axial strain along the subgrid vortex axis and is the same as a in the original model. Using the model spectrum (8) to evaluate the second integral in (13) and substituting the result into (16) yields

$$Re_\Delta X \Gamma(-1/3, X) - \Gamma(2/3, X) = 0, \quad (17)$$

where $X = k_c^2 \lambda_v^2$,

$$Re_\Delta = \frac{\bar{a}}{2\nu k_c^2} = \frac{\bar{a}}{3aX} \quad (18)$$

and $\Gamma(n, x)$ is the incomplete Gamma function. The rate-of-strain a is determined by calculating Re_Δ using the resolved rate-of-strain \bar{a} , solving equation (17) for X and finally using (18) to find a .

In practice, an asymptotic solution of equation (17) is used in order to avoid unnecessary evaluations of the Gamma function. The asymptotic solution is

$$X \sim Re_\Delta^{-3/2} \sum_{m=1}^6 c_m Re_\Delta^{-\frac{1}{2}(m-1)} \quad \text{as } Re_\Delta \rightarrow \infty, \quad (19)$$

where the coefficients c_m are listed in Table 1. The asymptotic

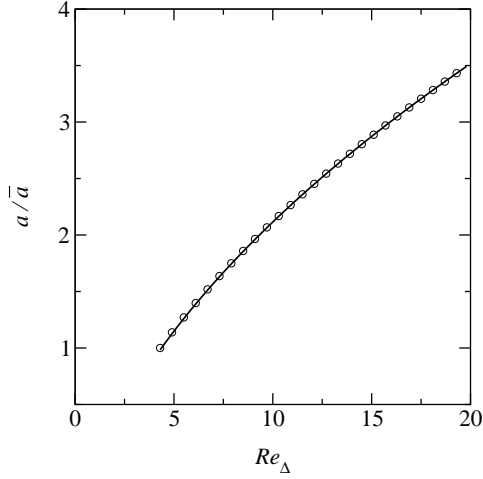


Figure 2: Asymptotic and direct numerical solutions of equation (17) (circles and solid line, respectively).

and direct numerical solutions of equation (17) are plotted together in Figure 2. For $Re_\Delta > 4.3011$, the error in the asymptotic solution is less than two percent. It is unnecessary to calculate X for $Re_\Delta < 4.3011$ because the external strain rate is then considered fully resolved, in which case $a = \bar{a}$.

The above algorithm completely resolves the grid dependence problem described earlier. Using the leading-order term in the asymptotic expansion and noting that the resolved rate-of-strain scales as $\bar{a} \sim \varepsilon^{1/3} \Delta^{-2/3}$ yields

$$\lambda_v^2 = \frac{X}{k_c^2} = \left(\frac{\bar{a}}{2v} \right)^{-3/2} k_c \sim \eta^2, \quad (20)$$

as required.

The above algorithm works when $\varepsilon_{sgs} = -\bar{S}_{ij}T_{ij} > 0$. This is true when the subgrid vortices are aligned with the principal extensional eigenvector. However, when the subgrid vortices are aligned with the resolved vorticity it is possible for $\varepsilon_{sgs} < 0$. In that case, it is impossible to find a solution because the integral for ε_{sgs} is positive. Several adhoc choices can be made. In the present simulations, the problem is avoided by using $|\bar{a}|$ in place of \bar{a} , as in equation (8).

The modification introduced by Chung & Pullin [3] is quite similar, but they make the additional assumption that

$$a = \left(\frac{\varepsilon}{15v} \right)^{1/2}, \quad (21)$$

which corresponds to isotropic flow, and essentially solve equation (16) without evaluating integrals of the form (13).

Results

The modified model is used to simulate turbulent temporal shear-layer flow in a rectangular prism. Cartesian coordinates (x, y, z) are oriented in the streamwise, cross-stream and spanwise directions, respectively, with corresponding components of velocity (u, v, w) . Periodic boundary conditions are imposed in the homogeneous streamwise and spanwise directions. The top and bottom of the domain are modelled as free-slip walls. A Fourier spectral collocation scheme is used in the homogeneous x and z directions. An eighth-order compact finite-difference scheme [7] is used in the inhomogeneous y direction. The grid spacing, Δ , is identical in each direction. All the simulations are run on the same 128×64^2 grid. The effective resolution Δ/η is

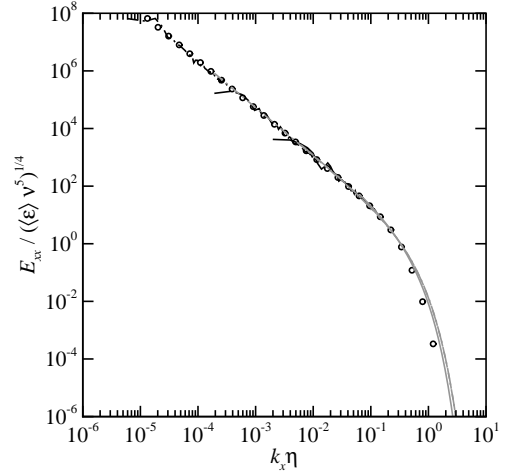


Figure 3: Resolved-scale (black) and subgrid-continued (grey) one-dimensional energy spectra for four different grid resolutions: $\Delta/\eta = 25$ (solid line), 259 (long-dash line) and 8264 (dot-dash line). Circles correspond to the empirical spectrum given by Pope [10]

controlled by changing the viscosity. Aliasing is minimised by calculating the nonlinear convective terms in skew-symmetric form [1]. A third-order variable-time-step Adams-Bashforth-Moulton scheme is used for temporal integration. The code was validated by computing solutions of the incompressible unsteady Stuart vortex (with the subgrid-scale model turned off and with suitably modified boundary conditions) [12].

The initial mean velocity profile is

$$\frac{\bar{u}}{\Delta U} = \frac{1}{2} \tanh\left(\frac{y}{d}\right), \quad (22)$$

where ΔU is the velocity difference across the layer and d is set to approximately 1.6Δ (this is the thinnest resolvable on the grid). This is perturbed by a random, three-dimensional, divergence-free disturbance.

One-dimensional energy spectra from simulations at three different effective resolutions are plotted in Figure 3. The spectra are defined such that $\int_0^\infty E_{ii}(k_x) dk_x = \langle u_i^2 \rangle$ [10], where the angled brackets denote a plane average and k_x is the wavenumber in the longitudinal x direction. Both the resolved-scale and subgrid-scale extensions are shown. Model estimates of the subgrid contributions to the resolved-scale spectrum have been included. The plane-averaged dissipation rate $\langle \varepsilon \rangle$, which is used to scale the spectra, is calculated from equation (12). Also included on this figure is the model spectrum developed by Pope [10], which is a good fit to a wide variety of spectral data.

The collapse of the spectra in Figure 3 indicates that the predicted subgrid extensions are independent of the effective resolution. There is excellent agreement between the simulation spectra and the empirical model in the inertial range. However, the subgrid extensions tend to overshoot the model spectrum near the viscous cut-off. This can be more clearly seen by plotting the compensated spectrum in log-linear coordinates, as is done in Figure 4. The simulations appear to produce spectra with an exponential cut-off of the form $\exp(-\beta k \eta)$ as originally proposed by Kraichnan [6], but the value of β is closer to 2 rather than the value of 5.2 that is commonly observed in experiments and simulations Pope [10].

Figure 5 shows spectra from three simulations which use differ-

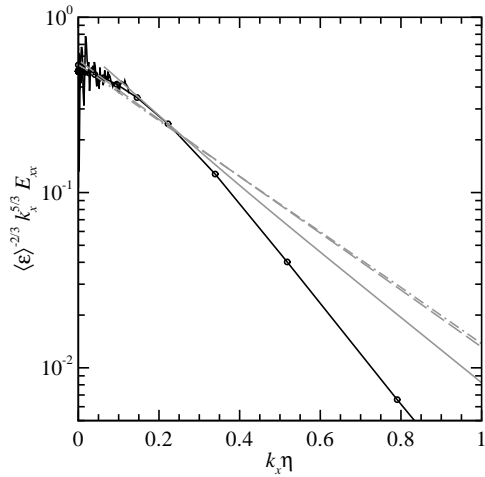


Figure 4: Resolved-scale (black) and subgrid-continued (grey) one-dimensional compensated energy spectra for four different grid resolutions: $\Delta/\eta = 25$ (solid line), 259 (long-dash line) and 8264 (dot-dash line). Lines with circles correspond to the empirical spectrum given by Pope [10]

ent elements of the modified and original model:

Simulation A is run using the mixed alignment model and equation (15) to estimate $\mathcal{X}_0 \varepsilon^{2/3}$.

Simulation B is run using the mixed alignment model and equation (9) to estimate $\mathcal{X}_0 \varepsilon^{2/3}$.

Simulation C is run using a single vortex aligned with the principal extensional eigenvector and equation (15) to estimate $\mathcal{X}_0 \varepsilon^{2/3}$.

These simulations are otherwise identical. The spectra from Simulations A and B are almost indiscernible, which indicates that equation (15) is at least as good as the original method of estimating $\mathcal{X}_0 \varepsilon^{2/3}$ using structure functions. Close inspection of the resolved-scale spectrum from Simulation C suggests that the largest resolved wave-numbers are somewhat more damped when the single-vortex alignment model is used instead of the mixed alignment model.

Conclusion

The model modifications presented in this paper produce estimates of the subgrid spectrum that are independent of the effective grid resolution. The modified model forces the energy transfer from resolved to subgrid scales ($-\bar{S}_{ij}T_{ij}$) to be the same as the estimate of the subgrid dissipation obtained by integrating the model spectrum, at least when the former quantity is positive. If a single-vortex alignment model is used, then $-\bar{S}_{ij}T_{ij} > 0$ and the two estimates of the subgrid dissipation are identical, but this comes at the expense of some additional damping at the largest resolved wave-numbers.

*

References

[1] Blaisdell, G. A., Spyropoulos, E. T. and Qin, J. H., The effect of the formulation of nonlinear terms on aliasing errors in spectral methods, *Appl. Numer. Math.*, **21**, 1996, 207–219.

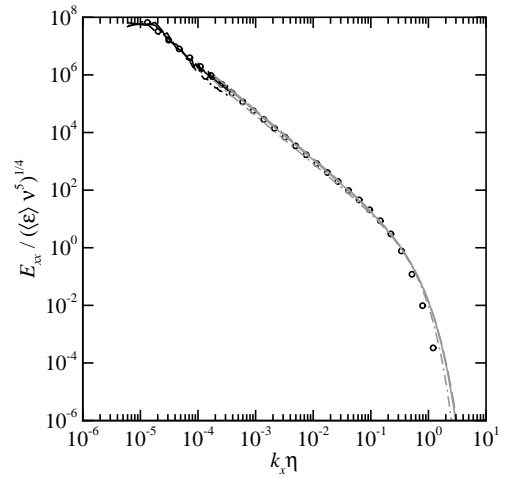


Figure 5: Resolved-scale (black) and subgrid-continued (grey) one-dimensional energy spectra for Simulations A (solid line), B (long-dash line) and C (dot-dash line). The effective resolution in each of these simulations is $\Delta/\eta = 8264$.

- [2] Chung, D. and Pullin, D. I., Large-eddy simulation and wall modelling of turbulent channel flow, *J. Fluid Mech.*, **631**, 2009, 281–309.
- [3] Chung, D. and Pullin, D. I., Direct numerical simulation and large-eddy simulation of stationary buoyancy-driven turbulence, *J. Fluid Mech.*, **643**, 2010, 279–308.
- [4] Hill, D. J., Pantano, C. and Pullin, D. I., Large-eddy simulation and multiscale modelling of a Richtmyer-Meshkov instability with reshock, *J. Fluid Mech.*, **557**, 2006, 29–61.
- [5] Kosovic, B., Pullin, D. I. and Samtaney, R., Subgrid-scale modeling for large-eddy simulations of compressible turbulence, *Phys. Fluids*, **14**, 2002, 1511–1522.
- [6] Kraichnan, R. H., The structure of isotropic turbulence at very high Reynolds number, *J. Fluid Mech.*, **5**, 1959, 497–543.
- [7] Lele, S. K., Compact finite difference schemes with spectral-like resolution, *J. Comp. Phys.*, **103**, 1992, 16–42.
- [8] Lesieur, M. and Metais, O., New trends in large-eddy simulations of turbulence, *Annu. Rev. Fluid Mech.*, **28**, 1996, 45–82.
- [9] Misra, A. and Pullin, D. I., A vortex-based subgrid stress model for large-eddy simulation, *Phys. Fluids*, **9**, 1997, 2443–2454.
- [10] Pope, S. B., *Turbulent Flows*, Cambridge University Press, 2000.
- [11] Pullin, D. I., A vortex-based model for the subgrid flux of a passive scalar, *Phys. Fluids*, **12**, 2000, 2311–2319.
- [12] Stuart, J. T., On finite amplitude oscillations in mixing layers, *J. Fluid Mech.*, **29**, 1967, 417–440.
- [13] Voekl, T., Pullin, D. I. and Chan, D. C., A physical-space version of the stretched-vortex subgrid-stress model for large-eddy simulation, *Phys. Fluids*, **12**, 2000, 1810–1825.